Sarm1 Gene Deficiency Attenuates Diabetic Peripheral Neuropathy in Mice

Yalan Cheng,[1] Jun Liu,[1] Yi Luan,[1] Zhiyuan Liu,[1] Hejin Lai,[1] Wuling Zhong,[1] Yale Yang,[1] Huimin Yu,[1] Ning Feng,[1] Hui Wang,[1] Rui Huang,[1] Zhishui He,[1] Menghong Yan,[1] Fang Zhang,[1] Yan-Gang Sun,[2] Hao Ying,[1] Feifan Guo,[1] and Qiwei Zhai[1,3]

Diabetes 2019;68:2120–2130 | https://doi.org/10.2337/db18-1233

Diabetic peripheral neuropathy (DPN) is the most common complication in both type 1 and type 2 diabetes, but any treatment toward the development of DPN is not yet available. Axon degeneration is an early feature of many peripheral neuropathies, including DPN. Delay of axon degeneration has beneficial effects on various neurodegenerative diseases, but its effect on DPN is yet to be elucidated. Deficiency of *Sarm1* significantly attenuates axon degeneration in several models, but the effect of *Sarm1* deficiency on DPN is still unclear. In this study, we show that *Sarm1* knockout mice exhibit normal glucose metabolism and pain sensitivity, and deletion of the *Sarm1* gene alleviates hypoalgesia in streptozotocin-induced diabetic mice. Moreover, *Sarm1* gene deficiency attenuates intraepidermal nerve fiber loss in footpad skin; alleviates axon degeneration, the change of g-ratio in sciatic nerves, and NAD^+ decrease; and relieves axonal outgrowth retardation of dorsal root ganglia from diabetic mice. In addition, *Sarm1* gene deficiency markedly diminishes the changes of gene expression profile induced by streptozotocin in the sciatic nerve, especially some abundant genes involved in neurodegenerative diseases. These findings demonstrate that *Sarm1* gene deficiency attenuates DPN in mice and suggest that slowing down axon degeneration is a potential promising strategy to combat DPN.

Diabetic peripheral neuropathy (DPN) is considered to be one of the most common chronic complications of diabetes and affects ~50% of patients with type 1 and type 2 diabetes (1,2). Moreover, DPN is also associated with substantial morbidity, including sleep disturbances, anxiety, depression, and susceptibility to foot or ankle fractures, ulceration, and lower-limb amputations (3–5). Clinical symptoms associated with DPN involve poor gait and balance, abnormal cold and/or heat sensation, hyperalgesia, allodynia, paresthesia, spontaneous pain, and numbness (6,7). At present, pregabalin, duloxetine, and even opioids, such as tapentadol, have received regulatory approval for the treatment of neuropathic pain associated with diabetes by the U.S. Food and Drug Administration, Health Canada, and the European Medicines Agency (8–10). However, use of these reagents can be limited by only relieving pain and has no beneficial impact on the natural history of DPN (5). There are no modifiable treatments for DPN other than lifestyle intervention and diabetes control (10). Therefore, seeking safe and effective treatments to alleviate DPN is still urgent.

The pathologic features of DPN are well characterized, including the polyol pathway hyperactivity, accumulation of advanced glycation end products (AGEs), diacylglycerol–protein kinase C (PKC) pathway activation, increased poly (ADP-ribose) polymerase (PARP) activity, enhanced modification of proteins with *N*-acetylglucosamine via the hexosamine pathway, oxidative stress, increased inflammation, and a reduction in neurotrophic factors (4,6,11). Aldose reductase is a key enzyme in the polyol pathway, and aldose reductase inhibitors show encouraging results in preclinical rodent studies (12,13). However, all clinical trials in humans using different aldose reductase inhibitors to treat

[1]CAS Key Laboratory of Nutrition, Metabolism and Food Safety, CAS Center for Excellence in Molecular Cell Sciences, Shanghai Institute of Nutrition and Health, Shanghai Institutes for Biological Sciences, University of Chinese Academy of Sciences, Chinese Academy of Sciences, Shanghai, China
[2]Institute of Neuroscience, Shanghai Institutes for Biological Sciences, Chinese Academy of Sciences, Shanghai, China
[3]School of Life Science and Technology, ShanghaiTech University, Shanghai, China
Corresponding author: Qiwei Zhai, qwzhai@sibs.ac.cn

Received 27 November 2018 and accepted 15 August 2019
This article contains Supplementary Data online at http://diabetes.diabetesjournals.org/lookup/suppl/doi:10.2337/db18-1233/-/DC1.

DPN failed in the U.S., Canada, and Europe (11). Although various preclinical trials targeting other pathologic features of DPN, including accumulation of AGEs, activation of PARP, PKC, and hexosamine pathways, oxidative stress, and inflammation, have shown some beneficial effects in animal models, all clinical trials aimed at altering the progressive course of DPN have failed (10). Therefore, novel strategies to treat DPN are extremely important.

Axon degeneration is a prominent early feature of most neurodegenerative disorders and the primary pathology in many peripheral neuropathies including DPN (14,15). Remarkably, axon degeneration is dramatically slowed in Wallerian degeneration slow (Wld^S) mice, a spontaneous mutant mouse strain, and Wld^S mice are resistant to various neurodegenerative diseases (14,16). Previously, we found that Wld^S mice are resistant to high-fat diet–induced or streptozotocin (STZ)–induced hyperglycemia (17). Therefore, it is not feasible to use Wld^S mice to study whether slowing down axon degeneration will have beneficial effects on DPN. SARM1 is highly conserved in humans, mice, *Drosophila*, and *Caenorhabditis elegans* (18,19). SARM1 was originally identified as a negative regulator of TRIF-dependent Toll-like receptor signaling (20). SARM1 has also been reported to interact with syndecan-2 and regulate neuronal morphology (21). Deletion of *Sarm1* provides a level of protection against axon degeneration that is comparable in strength to that provided by Wld^S (19). It has been reported that SARM1 activation triggers axon degeneration locally via NAD^+ destruction, and SARM1 possesses intrinsic NAD^+ cleavage activity that promotes pathological axonal degeneration (22,23). Genetic deletion of *Sarm1* in mice blocks Wallerian degeneration of sciatic nerve and cultured superior cervical ganglia and peripheral polyneuropathy induced by vincristine (19,24). However, whether deletion of *Sarm1* has an effect similar to that of Wld^S on glucose homeostasis is still unclear, and whether *Sarm1* deficiency has beneficial effects on DPN is yet to be elucidated.

In this study, we investigated whether $Sarm1^{-/-}$ mice are resistant to STZ-induced diabetes and DPN and the potential underlying molecular mechanisms. We found that $Sarm1^{-/-}$ mice are not resistant to STZ-induced diabetes but are resistant to STZ-induced DPN. Moreover, *Sarm1* gene deficiency markedly diminishes the changes of gene expression profile induced by STZ in sciatic nerves.

RESEARCH DESIGN AND METHODS

Animals

All animals were maintained and used in accordance with the guidelines of the Institutional Animal Care and Use Committee of the Institute for Nutritional Sciences.

$Sarm1^{-/-}$ mice with disruption of exons 3–6, generated as previously described (25), were obtained from The Jackson Laboratory. $Sarm1^{-/-}$ mice exhibit enhanced resistance to oxygen and glucose deprivation–induced neuronal death and have applications in studies of neurodegeneration (19,25). Male C57BL/6 mice were purchased from the Shanhai Laboratory Animals Center (SLAC).

Glucose and Insulin Tolerance Tests

Glucose tolerance tests and insulin tolerance tests were performed as described previously (26).

Immunoblotting

Immunoblotting was performed with antibodies against SARM1 (Thermo Fisher Scientific and Cell Signaling Technologies) or β-actin (Sigma-Aldrich).

RNA Isolation and Quantitative PCR

RNA extracted with TRIzol reagent was reverse-transcribed using M-MLV Reverse Transcriptase (Promega) with random hexamer primers. Quantitative PCR was performed using FastStart Universal SYBR Green Master (Roche) and the primers shown in Supplementary Table 1 and normalized to *36B4*.

Diabetic Mouse Model Induced by STZ

Ten-week-old male C57BL/6 and $Sarm1^{-/-}$ mice were injected intraperitoneally with 40 mg/kg/day STZ (Sigma-Aldrich) or an equivalent volume of vehicle for 5 consecutive days as described previously (17). The mice with a blood glucose level >250 mg/dL for 2 consecutive weeks were considered diabetic.

Behavioral Tests

A hot plate test was performed as previously described (27,28). Briefly, each mouse was habituated and then placed on the hot plate maintained at 50°C, 52°C, or 56°C. The latency for the mouse to lick its hind paw or jump was recorded. Individual measurements were repeated at least four times at a minimal 20-min interval. If the response did not occur within 60 s, the latency was recorded as 60 s.

The tail immersion test was done as previously reported (27). Briefly, the distal 30–40% of a mouse tail was immersed into a water bath at 50°C. The latency to tail flicking was measured. At least three readings were taken per animal at a minimal 15-min interval. If the response did not occur within 15 s, the latency was recorded as 15 s.

The von Frey test was performed as previously described (29). Animals were placed in transparent plastic domes on a metal mesh floor. After habituation, the threshold for hind paw withdrawal was measured by graded-strength von Frey monofilaments (Bioseb). A minimum of 10 min was set between two stimuli with different force to the same mouse. The cutoff force was 4 g.

Intraepidermal Nerve Fiber Density

Intraepidermal nerve fiber density (INFD) was assessed as described previously with minor modification (30). The longitudinal footpad sections were incubated overnight using antibody against PGP9.5 (Cedarlane Laboratories)

with 1:200 dilution and visualized by incubation with goat anti-rabbit antibody labeled with Alexa Fluor 488 (Jackson ImmunoResearch) with 1:500 dilution. Intraepidermal nerve fiber profiles were counted blindly, and the INFD data were presented as the mean number of fibers per linear millimeter of epidermis from four to six sections per mouse.

Transmission Electron Microscopy

The sciatic nerves were fixed overnight in cold 2.5% glutaraldehyde, then postfixed with 2% OsO_4 for 2 h, and embedded in epoxy resin after dehydration with ethanol and propylenoxide. The 70-nm ultrathin sections were prepared and stained with 4% uranyl acetate followed by lead citrate (31). At least two pictures were randomly taken using a transmission electron microscopy (JEOL Ltd.) from each sample for quantification of axon degeneration. Axon and myelinated fiber diameters were measured, and g-ratio was determined by dividing the axon diameter by the myelinated fiber diameter (31).

Measurement of NAD^+ Levels

NAD^+ levels were measured by the recycling assay as previously described (32).

Dorsal Root Ganglion Neuron Culture

Dorsal root ganglion (DRG) neuron culture was performed as previously described (33). After culturing for 48 h, the neurons were photographed, and the length of the longest axon was calculated by the distance from cell body to the

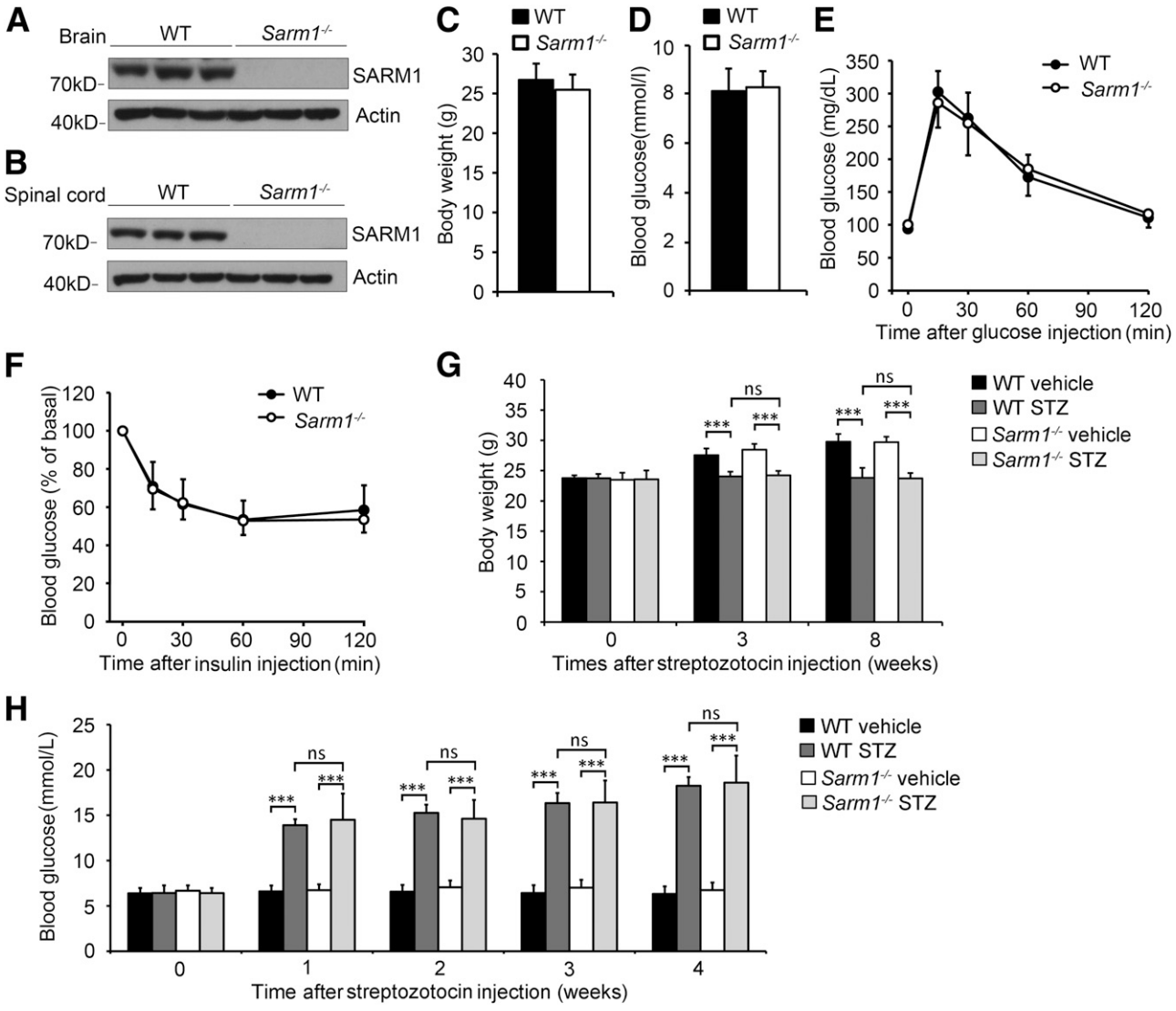

Figure 1—*Sarm1*$^{-/-}$ mice exhibit normal glucose metabolism. *A*: The protein levels of SARM1 in the brain of wild-type (WT) mice and *Sarm1*$^{-/-}$ mice. *B*: SARM1 protein levels in spinal cord of WT mice and *Sarm1*$^{-/-}$ mice. *C* and *D*: *Sarm1*$^{-/-}$ and WT mice exhibit similar body weight and blood glucose levels at 12 weeks of age. $n = 10$–12 for each group. *E* and *F*: Ten-week-old WT and *Sarm1*$^{-/-}$ mice were used for a glucose tolerance test (*E*) and insulin tolerance test (*F*). $n = 8$ for each group. *G* and *H*: WT and *Sarm1*$^{-/-}$ mice showed significantly decreased body weight and increased blood glucose after injection of STZ for the indicated times. $n = 8$–12 for each group. ***$P < 0.001$.

distal end of the longest axon. For each group, at least 3 batches of DRG neurons and >20 neurons for each batch were calculated.

High-Throughput RNA Sequencing

Spinal cords and sciatic nerves from wild-type and *Sarm1*$^{-/-}$ mice were dissected after 5-day consecutive injection with vehicle or STZ and in the subsequent 25 weeks to extract total RNA for RNA sequencing. Genes having a false discovery rate ≤0.001 and *abs*($\log_2$ fold change) ≥1 were considered as differentially expressed. Pathway analysis was performed in edgeR using Kyoto Encyclopedia of Genes and Genomes (KEGG) pathway enrichment analysis.

Statistical Analysis

Data are expressed as the mean ± SD of at least three independent experiments. Statistical significance was assessed by two-tailed unpaired Student *t* test or one-way ANOVA with Tukey multiple-comparison test. Differences were considered statistically significant at $P < 0.05$.

Data and Resource Availability

The data sets generated and/or analyzed during the current study are available from the corresponding author on reasonable request. The RNA-sequencing data generated and/or analyzed during the current study are available in the National Center for Biotechnology Information Sequence Read Archive repository (accession number PRJNA540413).

RESULTS

Sarm1 Gene–Deficient Mice Exhibit Normal Glucose Metabolism and Are Not Resistant to STZ-Induced Diabetes

To investigate whether *Sarm1* gene–deficient mice are suitable to study the role of SARM1 in DPN, we studied whether *Sarm1*$^{-/-}$ mice show normal glucose metabolism. *Sarm1* gene deficiency was confirmed by immunoblot. As shown in Fig. 1*A* and *B*, SARM1 protein was not detectable in brain and spinal cord in *Sarm1*$^{-/-}$ mice. Moreover, we found that the *Sarm1*$^{-/-}$ mice showed normal body weight and blood glucose level compared with wild-type mice (Fig. 1*C* and *D*). Then we detected the glucose and insulin tolerance and found that *Sarm1*$^{-/-}$ mice showed glucose and insulin tolerance similar to that of wild-type mice (Fig. 1*E* and *F*). These data show that *Sarm1* gene deficiency does not affect normal glucose metabolism in mice.

Wld^S mice show an obvious phenotype with markedly delayed axon degeneration, but previously, we found that *Wld*^{S} mice are resistant to STZ-induced diabetes and diet-induced hyperglycemia (17). Thus, *Wld*^{S} mice are not suitable to be directly used to study the function of *Wld*^{S} in DPN. To investigate whether *Sarm1*$^{-/-}$ mice are different from *Wld*^{S} mice, and potentially to be used to study the function of *Wld*^{S} in DPN, we detected whether *Sarm1*$^{-/-}$ mice are resistant to STZ-induced diabetes. Ten-week-old male mice were consecutively injected with 40 mg/kg/day STZ or vehicle intraperitoneally for 5 days, and the mice with a blood glucose level >250 mg/dL for 2 consecutive weeks after STZ injection were considered diabetic. As shown in Fig. 1*G*, we found STZ treatment downregulated body weight in both wild-type and *Sarm1*$^{-/-}$ mice, and wild-type and *Sarm1*$^{-/-}$ mice showed similar body weight when treated with or without STZ. Moreover, we found that *Sarm1*$^{-/-}$ mice showed significantly increased blood glucose after injection of STZ for 1 week and were confirmed to be diabetic after injection for 3 weeks as wild-type mice.

These data show that *Sarm1*$^{-/-}$ mice show normal glucose metabolism and can become diabetic, as with wild-type mice, after injection of STZ; thus, they are potentially suitable for studying the role of *Sarm1* deficiency in DPN.

Sarm1$^{-/-}$ Mice Show Normal Pain Sensitivity and INFD in Footpad Compared With Wild-Type Mice

DPN is often accompanied with hypoalgesia and loss of sensation (7). To investigate whether *Sarm1* gene–deficient mice are suitable to study the role of SARM1 in DPN, we also examined whether *Sarm1*$^{-/-}$ mice show normal pain sensitivity and INFD. The hot plate, tail immersion, and von Frey filament tests were used to measure pain sensitivity in mice. In a hot plate test and tail immersion test, the male *Sarm1*$^{-/-}$ mice showed normal withdrawal latency compared with wild-type mice (Fig. 2*A* and *B*). Meanwhile, the tactile allodynia threshold was also comparable in *Sarm1*$^{-/-}$ and wild-type mice as measured by paw withdrawal threshold upon exposure to von Frey filaments (Fig. 2*C*). These data show that there is no significant difference in pain sensitivity between *Sarm1*$^{-/-}$ and wild-type mice.

PGP9.5 immunostaining is widely used for the detection of small fiber neuropathy (34,35). We detected the INFD in the footpad skin of *Sarm1*$^{-/-}$ and wild-type mice and found the density of PGP9.5-positive intraepidermal nerve fibers was similar in *Sarm1*$^{-/-}$ and wild-type mice (Fig. 2*D*). This observation demonstrates that *Sarm1* gene deficiency does not affect the INFD of footpad skin under normal conditions. Taken together, these findings show that *Sarm1*$^{-/-}$ mice exhibit normal pain sensitivity and INFD in the footpad.

Sarm1 Deficiency Prevents Hypoalgesia in STZ-Induced Diabetic Mice

To investigate the potential role of SARM1 in DPN, *Sarm1*$^{-/-}$ and wild-type mice were consecutively injected with vehicle or 40 mg/kg/day STZ intraperitoneally for 5 days to induce diabetes. Twenty weeks later, we conducted the tail immersion latency test, hot plate test, and von Frey test to monitor their pain sensitivity. We found that STZ-induced diabetic mice showed significantly increased latency on a hot plate at 50, 52, and 55°C compared with the mice injected with vehicle (Fig. 3*A*). Although *Sarm1*$^{-/-}$ mice injected with STZ developed diabetes as did wild-type mice injected with STZ, diabetic

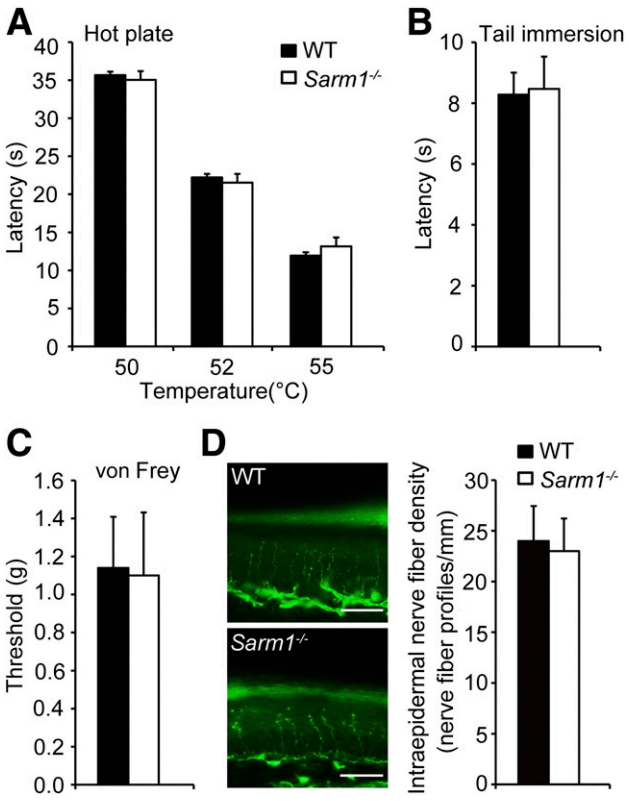

Figure 2—*Sarm1*$^{-/-}$ mice show normal pain sensitivity compared with wild-type (WT) mice. Responses to noxious thermal stimulation measured by hot plate test (*A*) and tail immersion latency test (*B*) were indistinguishable between *Sarm1*$^{-/-}$ and WT mice. n = 8–12 for each group. *C*: Tactile allodynia threshold was comparable in *Sarm1*$^{-/-}$ and WT mice as measured by paw withdrawal threshold upon exposure to von Frey filaments. n = 8–12 for each group. *D*: *Sarm1*$^{-/-}$ mice exhibit normal INFD. Representative images of intraepidermal nerve fiber profiles (left) and the quantification of INFD (right) in WT and *Sarm1*$^{-/-}$ mice at 10 weeks of age. Scale bars, 35 μm. n = 8–10 for each group.

Sarm1$^{-/-}$ mice showed a very significant decrease of latency on a hot plate at 50, 52, and 55°C compared with diabetic wild-type mice (Fig. 3*A*). Similarly, when measured by tail immersion test, diabetic wild-type mice showed significant upregulation of latency in a water bath at 50°C compared with normal wild-type mice, and diabetic *Sarm1*$^{-/-}$ mice showed a significant decrease of latency compared with diabetic wild-type mice (Fig. 3*B*). As expected, when measured by von Frey test, diabetic wild-type mice showed a markedly increased threshold upon exposure to von Frey filaments compared with normal wild-type mice, and diabetic *Sarm1*$^{-/-}$ mice showed a significant decrease of threshold compared with diabetic wild-type mice (Fig. 3*C*). Diabetes in the mice used in the above tests was confirmed by monitoring their blood glucose levels before the tests (Fig. 3*D*), and wild-type and *Sarm1*$^{-/-}$ mice showed similar body weight after being treated with or without STZ (Fig. 3*E*). These data demonstrate that *Sarm1* deficiency attenuates both thermal and mechanical hypoalgesia in diabetic mice.

Sarm1 Gene Deficiency Alleviates Diabetes-Induced Intraepidermal Nerve Fiber Loss

Diabetic hypoalgesia has been reported to be related to sensory nerve fiber dysfunction, such as intraepidermal nerve fiber loss (2,29). To further confirm that *Sarm1* gene deficiency has protective effects on DPN, we investigated whether knockout of *Sarm1* can attenuate diabetes-induced intraepidermal nerve fiber loss in footpad skin. As shown in Fig. 4*A* and *B*, the wild-type mice treated with STZ showed a dramatic decrease of INFD compared with the mice treated with vehicle. As expected, diabetic *Sarm1*$^{-/-}$ mice showed a significantly increased INFD compared with diabetic wild-type mice (Fig. 4*A* and *B*), although diabetic *Sarm1*$^{-/-}$ mice and wild-type mice showed similar blood glucose levels before the measurement of INFD (Fig. 4*C*). These data demonstrate that *Sarm1* gene deficiency can alleviate diabetes-induced intraepidermal nerve fiber loss and further confirmed the protective effects of *Sarm1* gene deficiency on DPN.

Sarm1 Gene Deficiency Alleviates Axon Degeneration in Sciatic Nerve and Axonal Outgrowth Retardation of DRG Neurons From Diabetic Mice

It has been reported that DPN is usually accompanied by axon degeneration in various nerves, such as sciatic nerve (36–38). To investigate whether *Sarm1* gene ablation has a protective effect on diabetic axon degeneration, transmission electron microscopy was used to observe the ultrastructure of sciatic nerve in diabetic mice. Typical cross-section images of normal axons containing uniform and dense myelination with structural integrity and degenerated axons with abnormal myelin structure are shown in Fig. 5*Ai* and 5*Aii–vi*, respectively, and representative cross-section images of axons from the sciatic nerve of *Sarm1*$^{-/-}$ mice and wild-type mice injected with vehicle or STZ are shown in Fig. 5*B*. The ratio of the physiological axon degeneration in sciatic nerves was comparable in *Sarm1*$^{-/-}$ mice and wild-type mice injected with vehicle (Fig. 5*B* and *C*). As expected, the ratio of axon degeneration in the sciatic nerve of *Sarm1*$^{-/-}$ mice treated with STZ was markedly decreased compared with that in wild-type mice treated with STZ (Fig. 5*B* and *C*). Moreover, g-ratio, a measurement for myelin sheath thickness and considered to indicate nerve conduction capacity (39), was significantly changed by STZ in wild-type mice (Fig. 5*D*), but not in *Sarm1*$^{-/-}$ mice (Fig. 5*E*). In addition, the g-ratio in wild-type and *Sarm1*$^{-/-}$ mice treated with STZ was significantly different (Fig. 5*E*). In addition, diabetic wild-type and *Sarm1*$^{-/-}$ mice showed similar NAD^+ levels in spinal cord, but *Sarm1* gene deficiency significantly alleviates diabetes-induced NAD^+ decrease in sciatic nerves (Fig. 5*G*). These data demonstrate that *Sarm1* gene ablation alleviates diabetes-induced axon degeneration, change of g-ratio, and NAD^+ decrease in sciatic nerves.

To further analyze the effect of *Sarm1* gene deficiency on axons, we cultured DRG neurons from normal and diabetic mice. Axonal outgrowth retardation was observed

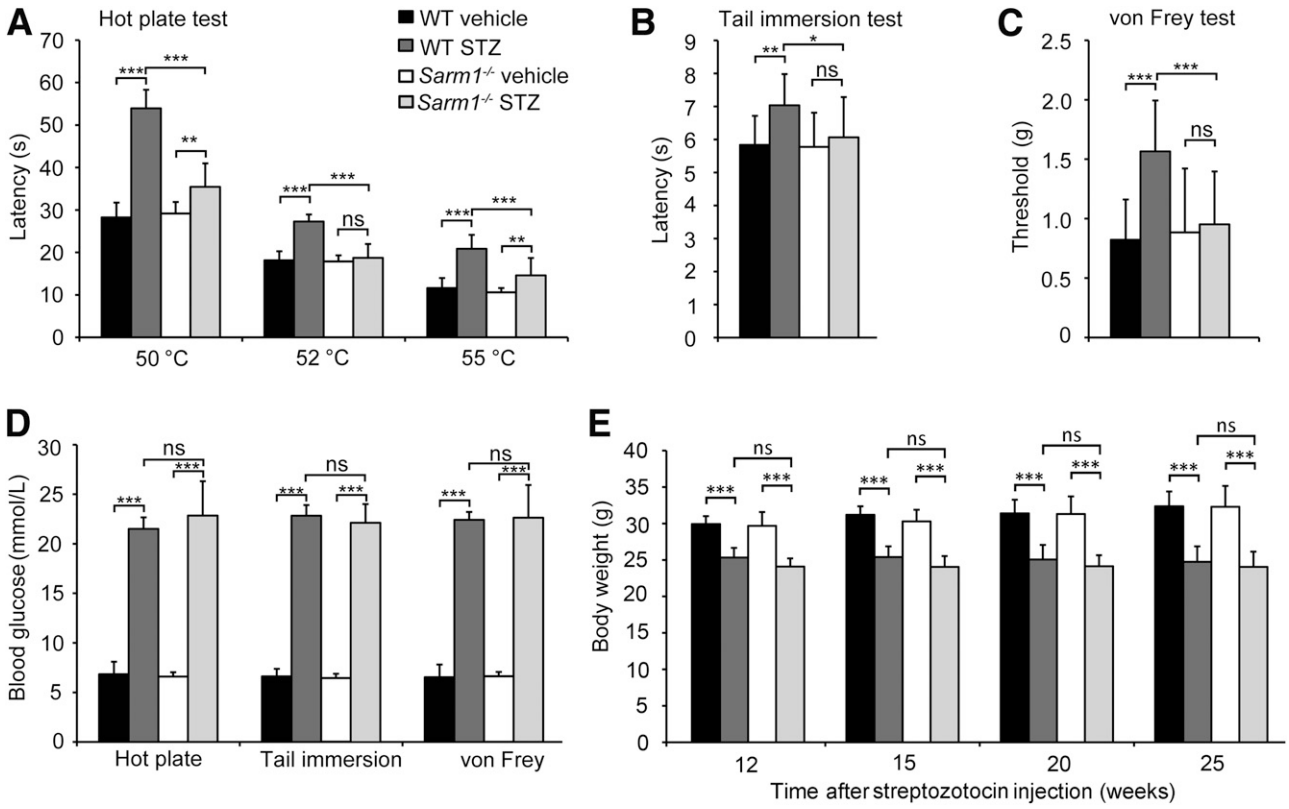

Figure 3—*Sarm1* gene deficiency alleviates hypoalgesia in diabetic mice. Response to noxious thermal stimulation measured by hot plate test (*A*) and tail immersion test (*B*) in wild-type (WT) and *Sarm1*$^{-/-}$ mice after 5-day consecutive injection with vehicle or STZ and for the subsequent 22 weeks. $n = 8–12$ for each group. *C*: Mechanical sensitivity was measured by paw withdrawal threshold upon exposure to von Frey filaments in mice after 5-day consecutive treatment with vehicle or STZ and subsequent 23 weeks. $n = 8–12$ for each group. *D*: The blood glucose levels of mice were measured before the indicated tests. $n = 8–12$ for each group. *E*: The body weights of mice were measured at the indicated time after STZ injection. $n = 8–12$ for each group. $^{*}P < 0.05$; $^{**}P < 0.01$; $^{***}P < 0.001$.

in DRG neurons from wild-type diabetic mice induced by STZ, and *Sarm1* gene deficiency can alleviate this effect (Fig. 5*H* and *I*).

SARM1 Protein Level Was Downregulated in Sciatic Nerve of Mice With DPN

To investigate the correlation of SARM1 with DPN, we measured the mRNA and protein levels of SARM1 in both spinal cord and sciatic nerve. We found that the mRNA levels of *Sarm1* in spinal cord and sciatic nerve were similar in mice treated with vehicle or STZ (Fig. 6*A*). The protein level of SARM1 in spinal cord was comparable in wild-type mice treated with vehicle or STZ, while the protein level of SARM1 in the sciatic nerve was decreased in mice with DPN induced by STZ (Fig. 6*B*). The sciatic nerves of diabetic mice had lower NAD^{+} levels than controls (Fig.

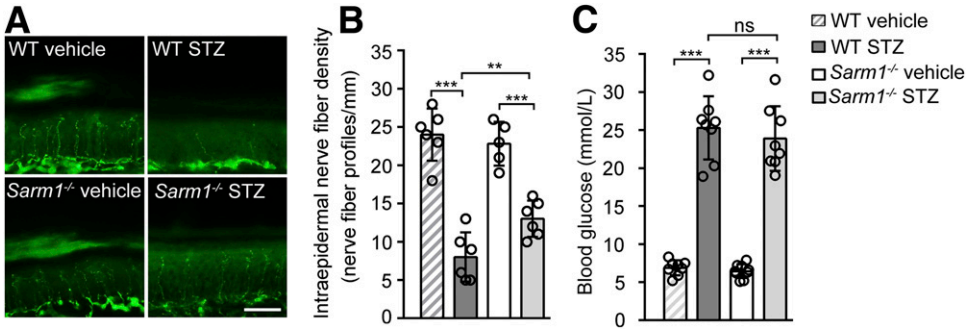

Figure 4—*Sarm1* gene deficiency attenuates intraepidermal nerve fiber loss in footpad skin of diabetic mice. Representative images of intraepidermal nerve fiber profiles (*A*) and the quantification of INFD (*B*) in wild-type (WT) and *Sarm1*$^{-/-}$ mice after 5-day injection with vehicle or STZ and for the subsequent 25 weeks. Scale bar, 35 μm; $n = 4–6$ for each group. *C*: The blood glucose levels of mice were detected before the measurement of INFD. $n = 8$ for each group. $^{**}P < 0.01$; $^{***}P < 0.001$.

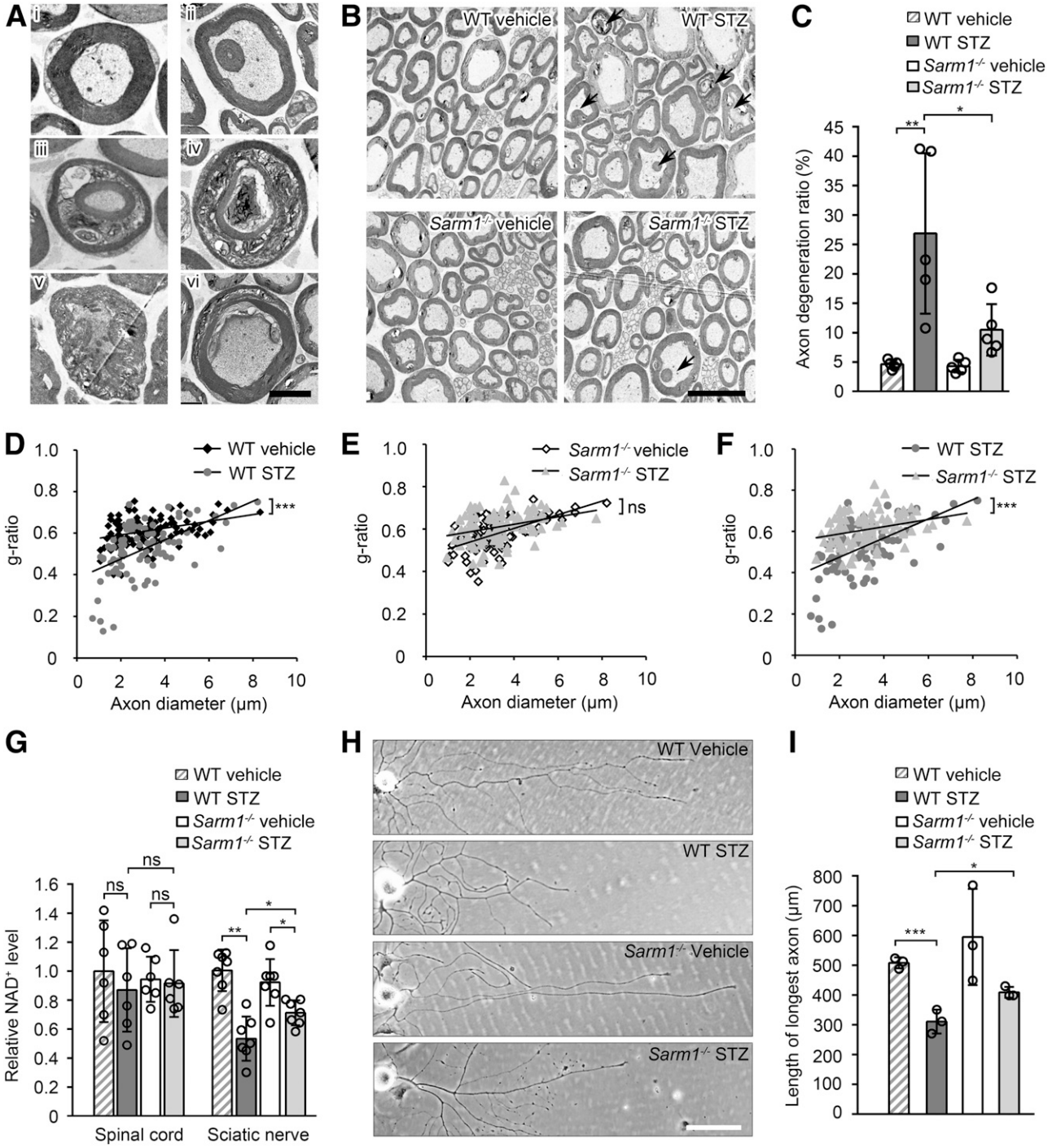

Figure 5—*Sarm1* gene deficiency alleviates diabetes-induced axon degeneration in sciatic nerve and axonal outgrowth retardation of DRG neurons from diabetic mice. *A*: Normal axons and various types of degenerated axons in sciatic nerve detected by transmission electron microscopy. *A*i: A normal axon with intact myelin sheath. *A*ii: Satellite myelinated axon within a bigger axon with normal axoplasm. *A*iii: Satellite myelinated axon with normal axoplasm within a bigger axon with abnormal axoplasm. *A*iv: Satellite myelinated axon with abnormal axoplasm within a bigger axon with abnormal axoplasm. *A*v: An axon with hypertrophic myelin sheath. *A*vi: A partially demyelinated axon. Scale bar, 2 μm. *B*: Representative electron micrographs of sciatic nerve in wild-type (WT) and *Sarm1*$^{-/-}$ mice after 5-day consecutive injection with vehicle or STZ and for the subsequent 25 weeks. Arrows indicate degenerated axons. Scale bar, 5 μm. *C*: The quantification of axon degeneration ratio in *B*. *D–F*: The scatter plot of g-ratio in sciatic nerve as described in *B*. $n = 5$ for each group. *G*: The NAD^+ levels of spinal cord and sciatic nerve in WT and *Sarm1*$^{-/-}$ mice after 5-day consecutive injection with vehicle or STZ and for the subsequent 25 weeks were measured. $n = 6$ for each group. *H* and *I*: The representative images and the quantification of the longest length of axons of cultured DRG neurons from WT and *Sarm1*$^{-/-}$ mice after 5-day consecutive injection with vehicle or STZ and for the subsequent 25 weeks. Scale bar, 100 μm. $n = 3$ for each group. *$P < 0.05$; **$P < 0.01$; ***$P < 0.001$.

5*G*), which would be due to the NAD^+ levels that are regulated by multiple pathways involved in its synthesis, consumption, or depletion (40). These data demonstrate that SARM1 protein levels can be downregulated in the sciatic nerve of diabetic mice, which might contribute to attenuate axon degeneration and DPN.

Deletion of *Sarm1* Diminishes the STZ-Induced Changes in Gene Expression Profile of Sciatic Nerve

To further confirm the effect of *Sarm1* deficiency on DPN, we investigated whether knockout of *Sarm1* can attenuate diabetes-induced gene expression in both spinal cord and sciatic nerve. As shown in Fig. 7*A*, both knockout of *Sarm1* and injection of STZ had a slight effect on gene expression profile in spinal cord. Injection of STZ in *Sarm1* gene–deficient mice had a modest effect in the spinal cord with 409 genes upregulated and 57 genes downregulated, and *Sarm1* gene deficiency also had a modest effect in the spinal cord of mice injected with STZ with 372 genes upregulated and 179 genes downregulated (Fig. 7*A*). Knockout of *Sarm1* had a modest effect on gene expression profile in sciatic nerves, with 440 genes upregulated and 223 genes downregulated, and injection of STZ had a relatively strong effect on gene expression profile in sciatic nerves, with 540 genes upregulated and 983 genes downregulated (Fig. 7*B*). Injection of STZ in *Sarm1* gene–deficient mice had a modest effect in sciatic nerves, with 296 genes upregulated and 471 genes downregulated, and *Sarm1* gene deficiency had a relatively strong effect in the spinal cord of mice injected with STZ, with 1,029 genes upregulated and 578 genes downregulated (Fig. 7*B*). In total, only 1.48% and 2.47% of the genes were significantly affected by STZ in spinal cords of wild-type and $Sarm1^{-/-}$ mice, respectively (Fig. 7*C*). Meanwhile, 8.05% of the genes were significantly affected by STZ in sciatic nerves of wild-type mice, and only 4.06% of the genes were significantly affected by STZ in sciatic nerves of $Sarm1^{-/-}$ mice (Fig. 7*D*), indicating that *Sarm1* gene deficiency can markedly attenuate the effect of STZ on gene expression in the sciatic nerve. The enriched KEGG pathway of differentially expressed genes in sciatic nerves of wild-type and $Sarm1^{-/-}$ mice injected with STZ is shown in Fig. 7*E*, and pathways involved in lipid metabolism and diabetes, including PI3K-Akt signaling in adipocytes, regulation of lipolysis in adipocytes, and AGE-RAGE signaling pathway in diabetic complications, appeared in the top 10 enriched pathways. In addition, the enrichment of differentially expressed genes in the sciatic nerve of wild-type and $Sarm1^{-/-}$ mice injected with STZ in human diseases is shown in Fig. 7*F*. The top four abundant genes enriched in neurodegenerative diseases were confirmed by quantitative PCR (Fig. 7*G* and Supplementary Table 2). These data show that *Sarm1* deficiency diminishes the STZ-induced changes in the gene expression profile of sciatic nerves, suggesting that deletion of *Sarm1* might attenuate DPN by diminishing the STZ-induced changes of gene expression in sciatic nerves or other peripheral nerves.

DISCUSSION

In this study, we observed that *Sarm1* gene deficiency has no significant effect on blood glucose level, glucose and insulin tolerance, pain sensitivity, and STZ-induced diabetes. Interestingly, deletion of the *Sarm1* gene alleviates hypoalgesia, intraepidermal nerve fiber loss in footpad skin, axon degeneration, and the change of g-ratio in the sciatic nerve in STZ-induced diabetic mice. *Sarm1* gene ablation also diminishes the STZ-induced changes of gene expression profile in sciatic nerves, especially some abundant genes involved in neurodegenerative diseases. These observations provide a novel therapeutic strategy to treat DPN.

It has been reported that chronic diabetes leads to distal axonopathy, with impaired sensory nerve function and degenerated peripheral axons (37,41). Consistent with a previous report that deletion of *Sarm1* delays axon degeneration (19), in this study, we show that *Sarm1* deficiency significantly alleviates hypoalgesia, intraepidermal nerve fiber loss, and axon degeneration in diabetic mice. However, we noted that the effects of *Sarm1* deficiency on intraepidermal nerve fiber loss and axon

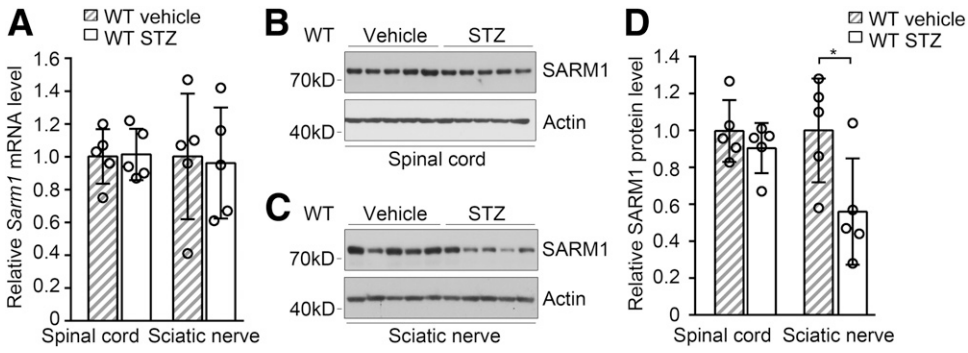

Figure 6— Injection of STZ downregulates SARM1 protein level in sciatic nerve. *A*: The mRNA level of *Sarm1* in spinal cord and sciatic nerve in wild-type (WT) mice after 5-day consecutive injection with vehicle or STZ and for the subsequent 25 weeks. $n = 6$ for each group. The protein level of SARM1 in spinal cord (*B* and *D*) and sciatic nerve (*C* and *D*) in WT mice as described in *A*. $n = 5$ for each group. $^*P < 0.05$.

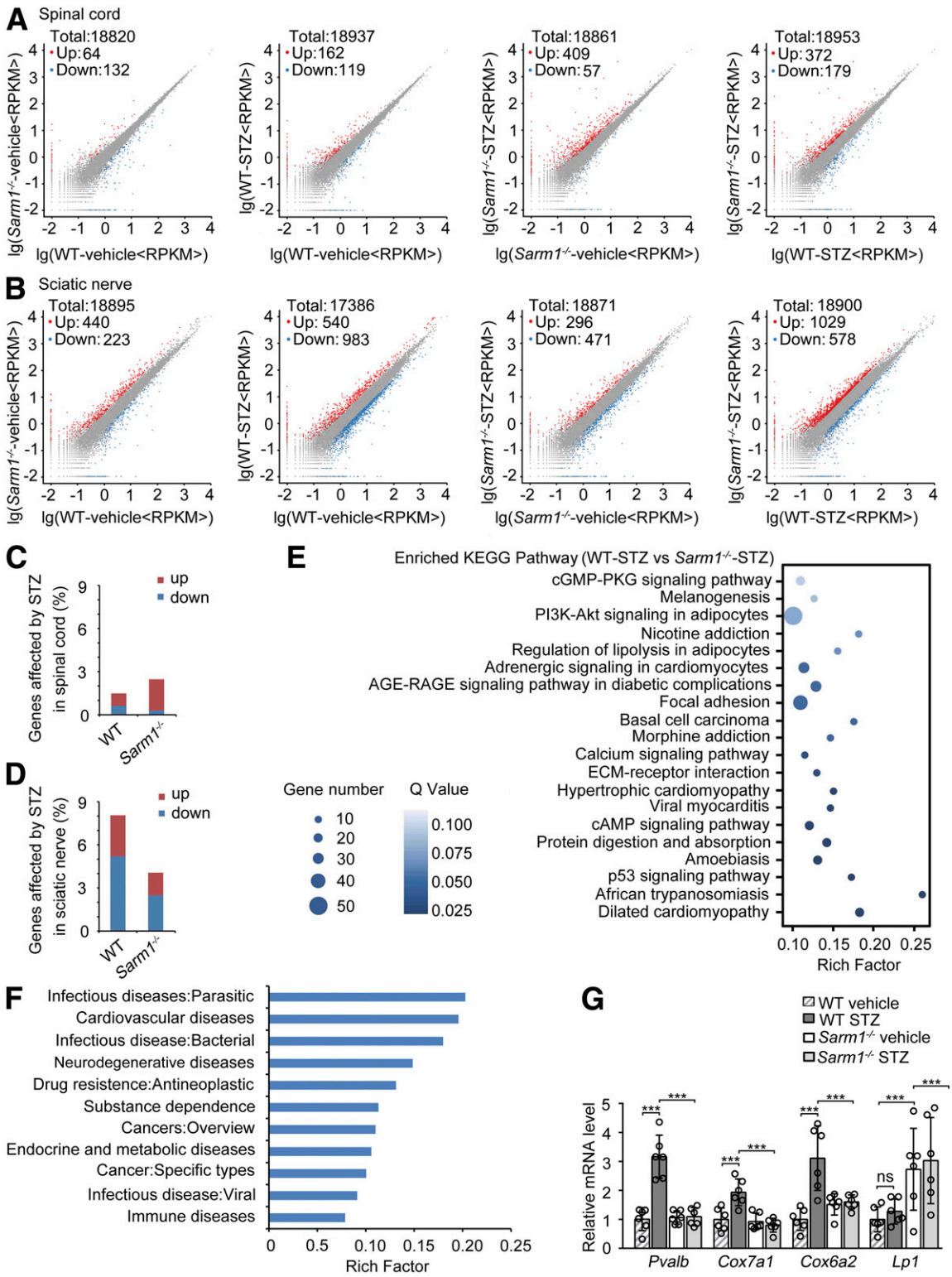

Figure 7—*Sarm1* gene deficiency diminishes the changes of gene expression profile induced by STZ in the sciatic nerve. Scatter plot comparing the differentially expressed genes detected by high-throughput sequencing in spinal cord (*A*) and sciatic nerve (*B*) between wild-type (WT) and *Sarm1*$^{-/-}$ mice after 5-day consecutive injection with vehicle or STZ and for the subsequent 25 weeks. *C* and *D*: The percentage of genes affected by STZ treatment in spinal cord (*C*) and sciatic nerve (*D*) of WT and *Sarm1*$^{-/-}$ mice as described in *A* and *B*. *E*: The top 20 significantly enriched KEGG pathway of the differentially expressed genes in sciatic nerve between WT and *Sarm1*$^{-/-}$ mice treated with STZ. *F*: The differentially expressed genes in sciatic nerve between WT and *Sarm1*$^{-/-}$ mice treated with STZ enriched in human diseases. *G*: Top four abundant genes enriched in neurodegenerative diseases in *F* were validated by quantitative PCR. $n = 6$ for each group. ***$P < 0.001$. ECM, extracellular matrix; RPKM, read per kilobase per million mapped reads.

degeneration in diabetic mice are not as dramatic as those on hypoalgesia. The discrepancy might be due to the fact that INFD and axon degeneration ratio in diabetic wild-type and *Sarm1*$^{-/-}$ mice are around the threshold to maintain normal peripheral pain sensitivity. Under this condition, a small but significant change of INFD and the axon degeneration ratio might lead to a dramatic change of peripheral pain sensitivity. These findings provide evidence that targeting axon degeneration, such as deletion of *Sarm1*, is a novel strategy to treat DPN. SARM1 is a multidomain adaptor molecule (19); future studies to reveal the key binding proteins of SARM1 involved in axon degeneration might provide new potential targets to treat DPN. In contrast, interfering peptides capable of interfering with protein–protein interactions are considered one of the next generation of drugs (42), and screening and identification of a peptide binding to SARM1 and inhibiting the function of SARM1 might have a therapeutic effect on DPN. Moreover, it has been reported that overexpression of Nmnat2, Nmant1, or Nmnat3, deletion of Phr1, or nicotinamide riboside supplementation can delay axon degeneration (23,43,44), and our findings also imply that the strategies to delay axon degeneration, other than deletion of *Sarm1*, such as increasing the activity of Nmnat2 or other Nmnats, inhibiting the E3 ligase Phr1, or nicotinamide riboside supplementation, may also have beneficial effects on DPN, although each strategy will lead to an effect distinct from SARM1 inhibition.

We found that many more genes in sciatic nerves than those in spinal cord were affected by diabetes, which is consistent with our observation of obvious axon degeneration in the sciatic nerve of diabetic mice. Similarly, it has been reported that the gene expression profile in the sciatic nerve of diabetic *db/db* mice was significantly changed, and axon degeneration in sciatic nerves of diabetic mice induced by STZ was dramatically increased (45,46). Moreover, metabolic dysfunction was also observed only in sciatic nerves of diabetic rats induced by STZ, but not in DRGs and trigeminal ganglia (47). As expected, we found *Sarm1* deficiency markedly reduced differentially expressed genes in diabetic mice. The genes affected by *Sarm1* deficiency in diabetic mice were enriched in several KEGG pathways, including AGE-RAGE signaling pathway and the calcium-signaling pathway. Both accumulation of AGEs and activation of PKC are pathologic features of DPN (4,11), and calcium signaling is usually linked to PKC signaling (48,49). Interestingly, we found that the genes affected by *Sarm1* deficiency in diabetic mice are significantly enriched in neurodegenerative diseases, and the top four abundant genes enriched in neurodegenerative diseases include *Pvalb*, *Cox7a1*, *Cox6a2*, and *Lp1*. Future studies on these four genes might provide new clues for the molecular mechanisms of DPN and axon degeneration alleviated by *Sarm1* deficiency.

Taken together, we found that *Sarm1* deficiency alleviates hypoalgesia, intraepidermal nerve fiber loss in footpad skin, axon degeneration, and the change of g-ratio in sciatic nerves and provides the potential underlying molecular mechanisms by showing the gene expression profile in both the spinal cord and sciatic nerve. Our findings provide strong evidence that targeting axon degeneration is a potential promising strategy to combat DPN.

Funding. This work was supported by grants from the National Natural Science Foundation of China (31630037, 91740103, 31470768, and 31670830), the National Key R&D Program of China (2018YFA0800603), the National Basic Research Program of China (2014CB542300), the Strategic Priority Research Program of the Chinese Academy of Sciences (XDB19000000), the Frontier Science of Chinese Academy of Sciences Key Research Projects (QYZDJ-SSW-SMC022), and the CAS/SAFEA International Partnership Program for Creative Research Teams.

Duality of Interest. No potential conflicts of interest relevant to this article were reported.

Author Contributions. Y.C., J.L., Z.L., H.L., W.Z., Y.Y., H. Yu, N.F., H.W., R.H., Z.H., M.Y., F.Z., Y.-G.S., H.Yi., F.G., and Q.Z. participated in data interpretation and revising the paper and approved the final version of the manuscript. The experiments were performed by Y.C. and J.L. The INFD was quantified by Y.C., Y.L., Z.L., H.L., and W.Z. The g-ratio was calculated by Y.C., Y.Y., H. Yu, and N.F. Y.C., Y.-G.S., H.Yi., F.G., and Q.Z. analyzed the data. This study was designed by Y.C. and Q.Z. Y.C. and Q.Z. wrote the paper. Q.Z. supervised the project. Q.Z. is the guarantor of this work and, as such, had full access to all of the data in the study and takes responsibility for the integrity of the data and the accuracy of the data analysis.

References

1. Boulton AJ, Vinik AI, Arezzo JC, et al.; American Diabetes Association. Diabetic neuropathies: a statement by the American Diabetes Association. Diabetes Care 2005;28:956–962

2. Shevalye H, Watcho P, Stavniichuk R, Dyukova E, Lupachyk S, Obrosova IG. Metanx alleviates multiple manifestations of peripheral neuropathy and increases intraepidermal nerve fiber density in Zucker diabetic fatty rats. Diabetes 2012;61:2126–2133

3. Gandhi RA, Marques JLB, Selvarajah D, Emery CJ, Tesfaye S. Painful diabetic neuropathy is associated with greater autonomic dysfunction than painless diabetic neuropathy. Diabetes Care 2010;33:1585–1590

4. Singh R, Kishore L, Kaur N. Diabetic peripheral neuropathy: current perspective and future directions. Pharmacol Res 2014;80:21–35

5. Boulton AJ, Kempler P, Ametov A, Ziegler D. Whither pathogenetic treatments for diabetic polyneuropathy? Diabetes Metab Res Rev 2013;29:327–333

6. Farmer KL, Li C, Dobrowsky RT. Diabetic peripheral neuropathy: should a chaperone accompany our therapeutic approach? Pharmacol Rev 2012;64:880–900

7. Edwards JL, Vincent AM, Cheng HT, Feldman EL. Diabetic neuropathy: mechanisms to management. Pharmacol Ther 2008;120:1–34

8. Waldfogel JM, Nesbit SA, Dy SM, et al. Pharmacotherapy for diabetic peripheral neuropathy pain and quality of life: a systematic review. Neurology 2017;88:1958–1967

9. Finnerup NB, Attal N, Haroutounian S, et al. Pharmacotherapy for neuropathic pain in adults: a systematic review and meta-analysis. Lancet Neurol 2015;14:162–173

10. Pop-Busui R, Boulton AJ, Feldman EL, et al. Diabetic neuropathy: a position statement by the American Diabetes Association. Diabetes Care 2017;40:136–154

11. Feldman EL, Nave KA, Jensen TS, Bennett DLH. New horizons in diabetic neuropathy: mechanisms, bioenergetics, and pain. Neuron 2017;93:1296–1313

12. Obrosova IG, Van Huysen C, Fathallah L, Cao XC, Greene DA, Stevens MJ. An aldose reductase inhibitor reverses early diabetes-induced changes in peripheral nerve function, metabolism, and antioxidative defense. FASEB J 2002;16:123–125

13. Cameron NE, Cotter MA, Basso M, Hohman TC. Comparison of the effects of inhibitors of aldose reductase and sorbitol dehydrogenase on neurovascular function, nerve conduction and tissue polyol pathway metabolites in streptozotocin-diabetic rats. Diabetologia 1997;40:271–281
14. Conforti L, Gilley J, Coleman MP. Wallerian degeneration: an emerging axon death pathway linking injury and disease. Nat Rev Neurosci 2014;15:394–409
15. Gerdts J, Summers DW, Milbrandt J, DiAntonio A. Axon self-destruction: new links among SARM1, MAPKs, and NAD+ metabolism. Neuron 2016;89:449–460
16. Mack TG, Reiner M, Beirowski B, et al. Wallerian degeneration of injured axons and synapses is delayed by a Ube4b/Nmnat chimeric gene. Nat Neurosci 2001;4:1199–1206
17. Wu J, Zhang F, Yan M, et al. WldS enhances insulin transcription and secretion via a SIRT1-dependent pathway and improves glucose homeostasis. Diabetes 2011;60:3197–3207
18. Mink M, Fogelgren B, Olszewski K, Maroy P, Csiszar K. A novel human gene (SARM) at chromosome 17q11 encodes a protein with a SAM motif and structural similarity to Armadillo/beta-catenin that is conserved in mouse, Drosophila, and Caenorhabditis elegans. Genomics 2001;74:234–244
19. Osterloh JM, Yang J, Rooney TM, et al. dSarm/Sarm1 is required for activation of an injury-induced axon death pathway. Science 2012;337:481–484
20. Carty M, Goodbody R, Schröder M, Stack J, Moynagh PN, Bowie AG. The human adaptor SARM negatively regulates adaptor protein TRIF-dependent Toll-like receptor signaling. Nat Immunol 2006;7:1074–1081
21. Chen CY, Lin CW, Chang CY, Jiang ST, Hsueh YP. Sarm1, a negative regulator of innate immunity, interacts with syndecan-2 and regulates neuronal morphology. J Cell Biol 2011;193:769–784
22. Essuman K, Summers DW, Sasaki Y, Mao X, DiAntonio A, Milbrandt J. The SARM1 toll/interleukin-1 receptor domain possesses intrinsic NAD^+ cleavage activity that promotes pathological axonal degeneration. Neuron 2017;93:1334–1343.e5
23. Gerdts J, Brace EJ, Sasaki Y, DiAntonio A, Milbrandt J. SARM1 activation triggers axon degeneration locally via NAD^+ destruction. Science 2015;348:453–457
24. Geisler S, Doan RA, Strickland A, Huang X, Milbrandt J, DiAntonio A. Prevention of vincristine-induced peripheral neuropathy by genetic deletion of SARM1 in mice. Brain 2016;139:3092–3108
25. Kim Y, Zhou P, Qian L, et al. MyD88-5 links mitochondria, microtubules, and JNK3 in neurons and regulates neuronal survival. J Exp Med 2007;204:2063–2074
26. Wang Y, Hu Y, Sun C, et al. Down-regulation of Risa improves insulin sensitivity by enhancing autophagy. FASEB J 2016;30:3133–3145
27. Sun YG, Zhao ZQ, Meng XL, Yin J, Liu XY, Chen ZF. Cellular basis of itch sensation. Science 2009;325:1531–1534
28. Caterina MJ, Leffler A, Malmberg AB, et al. Impaired nociception and pain sensation in mice lacking the capsaicin receptor. Science 2000;288:306–313
29. Drel VR, Mashtalir N, Ilnytska O, et al. The leptin-deficient (ob/ob) mouse: a new animal model of peripheral neuropathy of type 2 diabetes and obesity. Diabetes 2006;55:3335–3343
30. Stavniichuk R, Shevalye H, Lupachyk S, et al. Peroxynitrite and protein nitration in the pathogenesis of diabetic peripheral neuropathy. Diabetes Metab Res Rev 2014;30:669–678
31. Beirowski B, Babetto E, Golden JP, et al. Metabolic regulator LKB1 is crucial for Schwann cell-mediated axon maintenance. Nat Neurosci 2014;17:1351–1361
32. Hinman LM, Blass JP. An NADH-linked spectrophotometric assay for pyruvate dehydrogenase complex in crude tissue homogenates. J Biol Chem 1981;256:6583–6586
33. Li CL, Li KC, Wu D, et al. Somatosensory neuron types identified by high-coverage single-cell RNA-sequencing and functional heterogeneity. Cell Res 2016;26:83–102
34. Van Acker N, Ragé M, Sluydts E, et al. Automated PGP9.5 immunofluorescence staining: a valuable tool in the assessment of small fiber neuropathy? BMC Res Notes 2016;9:280
35. Koskinen M, Hietaharju A, Kyläniemi M, et al. A quantitative method for the assessment of intraepidermal nerve fibers in small-fiber neuropathy. J Neurol 2005;252:789–794
36. Cashman CR, Höke A. Mechanisms of distal axonal degeneration in peripheral neuropathies. Neurosci Lett 2015;596:33–50
37. Lennertz RC, Medler KA, Bain JL, Wright DE, Stucky CL. Impaired sensory nerve function and axon morphology in mice with diabetic neuropathy. J Neurophysiol 2011;106:905–914
38. Xu XF, Zhang DD, Liao JC, Xiao L, Wang Q, Qiu W. Galanin and its receptor system promote the repair of injured sciatic nerves in diabetic rats. Neural Regen Res 2016;11:1517–1526
39. Ikeda M, Oka Y. The relationship between nerve conduction velocity and fiber morphology during peripheral nerve regeneration. Brain Behav 2012;2:382–390
40. Cantó C, Menzies KJ, Auwerx J. NAD(+) metabolism and the control of energy homeostasis: a balancing act between mitochondria and the nucleus. Cell Metab 2015;22:31–53
41. Greene DA, Stevens MJ, Feldman EL. Diabetic neuropathy: scope of the syndrome. Am J Med 1999;107(2B):2S–8S
42. Bruzzoni-Giovanelli H, Alezra V, Wolff N, Dong CZ, Tuffery P, Rebollo A. Interfering peptides targeting protein-protein interactions: the next generation of drugs? Drug Discov Today 2018;23:272–285
43. Feng Y, Yan T, He Z, Zhai Q. Wld(S), Nmnats and axon degeneration–progress in the past two decades. Protein Cell 2010;1:237–245
44. Babetto E, Beirowski B, Russler EV, Milbrandt J, DiAntonio A. The Phr1 ubiquitin ligase promotes injury-induced axon self-destruction. Cell Rep 2013;3:1422–1429
45. Simon CM, Rauskolb S, Gunnersen JM, et al. Dysregulated IGFBP5 expression causes axon degeneration and motoneuron loss in diabetic neuropathy. Acta Neuropathol 2015;130:373–387
46. Terada M, Yasuda H, Kikkawa R. Delayed Wallerian degeneration and increased neurofilament phosphorylation in sciatic nerves of rats with streptozocin-induced diabetes. J Neurol Sci 1998;155:23–30
47. Freeman OJ, Unwin RD, Dowsey AW, et al. Metabolic dysfunction is restricted to the sciatic nerve in experimental diabetic neuropathy. Diabetes 2016;65:228–238
48. Lipp P, Reither G. Protein kinase C: the "masters" of calcium and lipid. Cold Spring Harb Perspect Biol 2011;3:a004556
49. Geraldes P, King GL. Activation of protein kinase C isoforms and its impact on diabetic complications. Circ Res 2010;106:1319–1331